Can time-resolved NIRS provide the sensitivity to detect brain activity during motor imagery consistently?

Androu Abdalmalak,[1,2*] Daniel Milej,[1,2] Mamadou Diop,[1,2] Mahsa Shokouhi,[1,2] Lorina Naci,[3] Adrian M. Owen,[3] and Keith St. Lawrence[1,2]

[1]*Department of Medical Biophysics, Western University, London, ON, Canada*
[2]*Imaging Division, Lawson Health Research Institute, London, ON, Canada*
[3]*Brain and Mind Institute, Western University, London, ON, Canada*
[*]*aabdalma@uwo.ca*

Abstract: Previous functional magnetic resonance imaging (fMRI) studies have shown that a subgroup of patients diagnosed as being in a vegetative state are aware and able to communicate by performing a motor imagery task in response to commands. Due to the fMRI's cost and accessibility, there is a need for exploring different imaging modalities that can be used at the bedside. A promising technique is functional near infrared spectroscopy (fNIRS) that has been successfully applied to measure brain oxygenation in humans. Due to the limited depth sensitivity of continuous-wave NIRS, time-resolved (TR) detection has been proposed as a way of enhancing the sensitivity to the brain, since late arriving photons have a higher probability of reaching the brain. The goal of this study was to assess the feasibility and sensitivity of TR fNIRS in detecting brain activity during motor imagery. Fifteen healthy subjects were recruited in this study, and the fNIRS results were validated using fMRI. The change in the statistical moments of the distribution of times of flight (number of photons, mean time of flight and variance) were calculated for each channel to determine the presence of brain activity. The results indicate up to an 86% agreement between fMRI and TR-fNIRS and the sensitivity ranging from 64 to 93% with the highest value determined for the mean time of flight. These promising results highlight the potential of TR-fNIRS as a portable brain computer interface for patients with disorder of consciousness.

OCIS codes: (170.2655) Functional monitoring and imaging; (170.6920) Time-resolved imaging; (170.0110) Imaging systems; (120.3890) Medical optics instrumentation.

References and links

1. D. Fernández-Espejo and A. M. Owen, "Detecting awareness after severe brain injury," Nat. Rev. Neurosci. **14**(11), 801–809 (2013).
2. D. Fernández-Espejo, L. Norton, and A. M. Owen, "The Clinical Utility of fMRI for Identifying Covert Awareness in the Vegetative State: a Comparison of Sensitivity Between 3T and 1.5T," PLoS One **9**(4), e95082 (2014).
3. S. Laureys, A. M. Owen, and N. D. Schiff, "Brain function in coma, vegetative state, and related disorders," Lancet Neurol. **3**(9), 537–546 (2004).
4. A. M. Owen, M. R. Coleman, M. Boly, M. H. Davis, S. Laureys, and J. D. Pickard, "Detecting Awareness in the Vegetative State," Science **313**(5792), 1402 (2006).
5. M. M. Monti, A. Vanhaudenhuyse, M. R. Coleman, M. Boly, J. D. Pickard, L. Tshibanda, A. M. Owen, and S. Laureys, "Willful modulation of brain activity in disorders of consciousness," N. Engl. J. Med. **362**(7), 579–589 (2010).
6. F. Scholkmann, S. Kleiser, A. J. Metz, R. Zimmermann, J. Mata Pavia, U. Wolf, and M. Wolf, "A review on continuous wave functional near-infrared spectroscopy and imaging instrumentation and methodology," Neuroimage **85**(Pt 1), 6–27 (2014).
7. M. Ferrari and V. Quaresima, "A brief review on the history of human functional near-infrared spectroscopy (fNIRS) development and fields of application," Neuroimage **63**(2), 921–935 (2012).
8. S. Coyle, T. Ward, C. Markham, and G. McDarby, "On the suitability of near-infrared (NIR) systems for next-generation brain-computer interfaces," Physiol. Meas. **25**(4), 815–822 (2004).
9. L. Holper and M. Wolf, "Single-trial classification of motor imagery differing in task complexity: a functional near-infrared spectroscopy study," J. Neuroeng. Rehabil. **8**(34), 34 (2011).
10. N. Naseer and K.-S. Hong, "fNIRS-based brain-computer interfaces : a review," Front. Hum. Neurosci. **9**(3), 1–15 (2015).
11. N. Naseer and K. S. Hong, "Classification of functional near-infrared spectroscopy signals corresponding to

the right- and left-wrist motor imagery for development of a brain-computer interface," Neurosci. Lett. **553**, 84–89 (2013).
12. M. Naito, Y. Michioka, K. Ozawa, Y. Ito, M. Kiguchi, and T. Kanazawa, "A communication means for totally locked-in ALS patients based on changes in cerebral blood volume measured with near-infrared light," IEICE Trans. Inf. Syst. **E90–D**(7), 1028–1037 (2007).
13. G. Gallegos-Ayala, A. Furdea, K. Takano, C. A. Ruf, H. Flor, and N. Birbaumer, "Brain communication in a completely locked-in patient using bedside near-infrared spectroscopy," Neurology **82**(21), 1930–1932 (2014).
14. A. M. Kempny, L. James, K. Yelden, S. Duport, S. Farmer, E. D. Playford, and A. P. Leff, "Functional near infrared spectroscopy as a probe of brain function in people with prolonged disorders of consciousness," Neuroimage Clin. **12**, 312–319 (2016).
15. D. Milej, D. Janusek, A. Gerega, S. Wojtkiewicz, P. Sawosz, J. Treszczanowicz, W. Weigl, and A. Liebert, "Optimization of the method for assessment of brain perfusion in humans using contrast-enhanced reflectometry: multidistance time-resolved measurements," J. Biomed. Opt. **20**(10), 106013 (2015).
16. I. Tachtsidis and F. Scholkmann, "Erratum: Publisher's note: False positives and false negatives in functional near-infrared spectroscopy: issues, challenges, and the way forward," Neurophotonics **3**(3), 039801 (2016).
17. E. Kirilina, A. Jelzow, A. Heine, M. Niessing, H. Wabnitz, R. Brühl, B. Ittermann, A. M. Jacobs, and I. Tachtsidis, "The physiological origin of task-evoked systemic artefacts in functional near infrared spectroscopy," Neuroimage **61**(1), 70–81 (2012).
18. M. A. Yücel, J. Selb, C. M. Aasted, P.-Y. Lin, D. Borsook, L. Becerra, and D. A. Boas, "Mayer waves reduce the accuracy of estimated hemodynamic response functions in functional near-infrared spectroscopy," Biomed. Opt. Express **7**(8), 3078–3088 (2016).
19. R. Sitaram, H. Zhang, C. Guan, M. Thulasidas, Y. Hoshi, A. Ishikawa, K. Shimizu, and N. Birbaumer, "Temporal classification of multichannel near-infrared spectroscopy signals of motor imagery for developing a brain-computer interface," Neuroimage **34**(4), 1416–1427 (2007).
20. L. Holper, N. Kobashi, D. Kiper, F. Scholkmann, M. Wolf, and K. Eng, "Trial-to-trial variability differentiates motor imagery during observation between low versus high responders: a functional near-infrared spectroscopy study," Behav. Brain Res. **229**(1), 29–40 (2012).
21. L. Holper, D. E. Shalóm, M. Wolf, and M. Sigman, "Understanding inverse oxygenation responses during motor imagery: a functional near-infrared spectroscopy study," Eur. J. Neurosci. **33**(12), 2318–2328 (2011).
22. M. Kacprzak, A. Liebert, P. Sawosz, N. Żolek, and R. Maniewski, "Time-resolved optical imager for assessment of cerebral oxygenation," J. Biomed. Opt. **12**(3), 034019 (2007).
23. R. R. Alfano, S. G. Demos, P. Galland, S. K. Gayen, Y. Guo, P. P. Ho, X. Liang, F. Liu, L. Wang, Q. Z. Wang, and W. B. Wang, "Time-resolved and nonlinear optical imaging for medical applications," Ann. N. Y. Acad. Sci. **838**(1 ADVANCES IN O), 14–28 (1998).
24. M. Diop and K. St. Lawrence, "Improving the depth sensitivity of time-resolved measurements by extracting the distribution of times-of-flight," Biomed. Opt. Express **4**(3), 447–459 (2013).
25. M. Diop and K. St. Lawrence, "Deconvolution method for recovering the photon time-of-flight distribution from time-resolved measurements," Opt. Lett. **37**(12), 2358–2360 (2012).
26. D. Milej, A. Abdalmalak, D. Janusek, M. Diop, A. Liebert, and K. St. Lawrence, "Time-resolved subtraction method for measuring optical properties of turbid media," Appl. Opt. **55**(7), 1507–1513 (2016).
27. D. Milej, A. Abdalmalak, P. McLachlan, M. Diop, A. Liebert, and K. St. Lawrence, "Subtraction-based approach for enhancing the depth sensitivity of time-resolved NIRS," Biomed. Opt. Express **7**(11), 4514–4526 (2016).
28. R. Re, D. Contini, M. Turola, L. Spinelli, L. Zucchelli, M. Caffini, R. Cubeddu, and A. Torricelli, "Multi-channel medical device for time domain functional near infrared spectroscopy based on wavelength space multiplexing," Biomed. Opt. Express **4**(10), 2231–2246 (2013).
29. D. Milej, A. Gerega, M. Kacprzak, P. Sawosz, W. Weigl, R. Maniewski, and A. Liebert, "Time-resolved multi-channel optical system for assessment of brain oxygenation and perfusion by monitoring of diffuse reflectance and fluorescence," Opto-Electron. Rev. **22**(1), 55–67 (2014).
30. A. Liebert, H. Wabnitz, J. Steinbrink, H. Obrig, M. Möller, R. Macdonald, A. Villringer, and H. Rinneberg, "Time-resolved multidistance near-infrared spectroscopy of the adult head: intracerebral and extracerebral absorption changes from moments of distribution of times of flight of photons," Appl. Opt. **43**(15), 3037–3047 (2004).
31. S. de Vries and T. Mulder, "Motor imagery and stroke rehabilitation: a critical discussion," J. Rehabil. Med. **39**(1), 5–13 (2007).
32. A. Abdalmalak, D. Milej, M. Diop, L. Naci, A. M. Owen, and K. St. Lawrence, "Assessing the feasibility of time-resolved fNIRS to detect brain activity during motor imagery," Proc. SPIE **9690**, 969002 (2016).
33. M. Boly, M. R. Coleman, M. H. Davis, A. Hampshire, D. Bor, G. Moonen, P. A. Maquet, J. D. Pickard, S. Laureys, and A. M. Owen, "When thoughts become action: an fMRI paradigm to study volitional brain activity in non-communicative brain injured patients," Neuroimage **36**(3), 979–992 (2007).
34. R. M. Gibson, D. Fernández-Espejo, L. E. Gonzalez-Lara, B. Y. Kwan, D. H. Lee, A. M. Owen, and D. Cruse, "Multiple tasks and neuroimaging modalities increase the likelihood of detecting covert awareness in patients with disorders of consciousness," Front. Hum. Neurosci. **8**(950), 950 (2014).
35. M. Diop, K. M. Tichauer, J. T. Elliott, M. Migueis, T.-Y. Lee, and K. St. Lawrence, "Comparison of time-resolved and continuous-wave near-infrared techniques for measuring cerebral blood flow in piglets," J. Biomed. Opt. **15**(5), 057004 (2010).
36. M. Diop, K. M. Tichauer, J. T. Elliott, M. Migueis, T.-Y. Lee, and K. St. Lawrence, "Time-resolved near-infrared technique for bedside monitoring of absolute cerebral blood flow," Proc. SPIE **7555**, 75550Z (2010).

37. A. Liebert, H. Wabnitz, D. Grosenick, M. Möller, R. Macdonald, and H. Rinneberg, "Evaluation of optical properties of highly scattering media by moments of distributions of times of flight of photons," Appl. Opt. **42**(28), 5785–5792 (2003).
38. F. Scholkmann, S. Spichtig, T. Muehlemann, and M. Wolf, "How to detect and reduce movement artifacts in near-infrared imaging using moving standard deviation and spline interpolation," Physiol. Meas. **31**(5), 649–662 (2010).
39. S. M. Liao, N. M. Gregg, B. R. White, B. W. Zeff, K. A. Bjerkaas, T. E. Inder, and J. P. Culver, "Neonatal hemodynamic response to visual cortex activity: high-density near-infrared spectroscopy study," J. Biomed. Opt. **15**(2), 026010 (2010).
40. M. Ahn and S. C. Jun, "Performance variation in motor imagery brain-computer interface: a brief review," J. Neurosci. Methods **243**, 103–110 (2015).
41. A. Guillot, C. Collet, V. A. Nguyen, F. Malouin, C. Richards, and J. Doyon, "Brain activity during visual versus kinesthetic imagery: an fMRI study," Hum. Brain Mapp. **30**(7), 2157–2172 (2009).
42. S. M. Coyle, T. E. Ward, and C. M. Markham, "Brain-computer interface using a simplified functional near-infrared spectroscopy system," J. Neural Eng. **4**(3), 219–226 (2007).
43. L. Holper and M. Wolf, "Motor imagery in response to fake feedback measured by functional near-infrared spectroscopy," Neuroimage **50**(1), 190–197 (2010).
44. T. Hanakawa, I. Immisch, K. Toma, M. A. Dimyan, P. Van Gelderen, and M. Hallett, "Functional properties of brain areas associated with motor execution and imagery," J. Neurophysiol. **89**(2), 989–1002 (2003).
45. F. P. de Lange, P. Hagoort, and I. Toni, "Neural topography and content of movement representations," J. Cogn. Neurosci. **17**(1), 97–112 (2005).
46. L. Gagnon, R. J. Cooper, M. A. Yücel, K. L. Perdue, D. N. Greve, and D. A. Boas, "Short separation channel location impacts the performance of short channel regression in NIRS," Neuroimage **59**(3), 2518–2528 (2012).
47. A. Torricelli, D. Contini, A. Pifferi, M. Caffini, R. Re, L. Zucchelli, and L. Spinelli, "Time domain functional NIRS imaging for human brain mapping," Neuroimage **85**(Pt 1), 28–50 (2014).
48. A. D. Mora, E. Martinenghi, D. Contini, A. Tosi, G. Boso, T. Durduran, S. Arridge, F. Martelli, A. Farina, A. Torricelli, and A. Pifferi, "Fast silicon photomultiplier improves signal harvesting and reduces complexity in time-domain diffuse optics," Opt. Express **23**(11), 13937–13946 (2015).

1. Introduction

Consciousness can be empirically defined as the state of being awake and aware of oneself and one's surroundings [1]. While determining wakefulness is a relatively simple task, assessing awareness is not trivial. In clinical scenarios, the presence of awareness is measured by the ability to follow commands, either behaviourally or verbally [2]. Because of this reliance on observable responses, a subset of patients who retain some cognitive function but are unable to follow commands are frequently diagnosed incorrectly as suffering from unresponsive wakefulness syndrome (UWS) or what is commonly referred to as a vegetative state [1,3].

An objective approach to assessing cognitive function without relying on behavioral assessment is by functional neuroimaging. In 2006, functional magnetic resonance imaging (fMRI) was used to demonstrate that a patient who fulfilled all the clinical diagnostic criteria of UWS exhibited command-driven brain activity, indicating that she was in fact aware [4]. Using a motor imagery (MI) task (i.e. imagine playing tennis) and by activating the brain regions associated with motion planning (i.e. supplementary motor area (SMA) and premotor cortex (PMC)), the patient was able to follow commands and produce brain activity that was indistinguishable from that of healthy volunteers [4]. This finding has revolutionized studies involving patients with disorders of consciousness (DOC), with various follow up studies demonstrating the ability to communicate with VS/UWS patients using fMRI [5].

While fMRI provides global coverage of brain activity, its accessibility, cost and exclusion criteria make it impractical for long-term use with DOC patients. Clearly, there is a need for portable and low-cost alternatives that could be used at the bedside of patients. A promising technology is functional near-infrared spectroscopy (NIRS), which can detect changes in regional brain activity due to its sensitivity to the concurrent changes in oxy- and deoxy-hemoglobin concentrations [6,7]. Coyle and colleagues were the first to demonstrate the utility of fNIRS as a brain computer interface (BCI) by asking participants to imagine squeezing and releasing a soft ball [8]. Further studies have been conducted using other MI tasks such as imagining simple or complex sequence of finger tapping [9] and imagining wrist flexion [10,11]. This approach has been used as a tool to communicate with totally locked-in amyotrophic lateral sclerosis patients [12,13],

although it was only successful in 40% of cases. Only one study to date has investigated the application of fNIRS to DOC [14]. A significant difference between hemispheric oxy-hemoglobin responses during MI of squeezing a ball was found in a group of patients diagnosed with either UWS or minimally conscious state. However, the effect was only significant at the group-wise level and an inverted oxy-hemoglobin response was reported for several participants (both controls and patients). Although promising, the inconsistencies in these patient studies highlight the need to explore alternative fNIRS methods and MI tasks that together can provide a reliable BCI that works on individual participants and thus allow for this technology to be successfully translated to DOC patients.

A major challenge with fNIRS is its limited depth sensitivity [15], which can reduce its ability to detect brain activity and makes it prone to signal contamination from extra-cerebral tissue. Variations in scalp blood flow and oxygenation due to systemic factors, such as fluctuations in arterial blood pressure, can mask brain activity by increasing signal variability and lead to false activation if systemic effects are synchronized with the task paradigm [16–18]. In terms of detecting MI activation, these confounders present an even a greater challenge considering the reported higher inter-subject variability and smaller signal change compared to motor execution tasks [19–21]. One approach for enhancing depth sensitivity is time-resolved (TR) detection [22–25], which records the arrival times of individual photons to build a distribution of times of flight (DTOF) [26,27]. Depth sensitivity is based on the principle that photons that only interrogate superficial tissue will have shorter time of flight compared to late-arriving photons that have a higher probability of reaching the brain. Depth information can be extracted from a DTOF using time bins centred on late arrival times or by calculating the statistical moments (area under the curve, mean time of flight, and variance) [28–30]. The area under the curve reflects total light intensity, analogous to conventional continuous-wave NIRS, whereas the higher moments have greater sensitivity to late-arriving photons because of the positive skewness of DTOFs.

The aim of this study was to investigate the feasibility of using a simple four-channel TR-NIRS system to detect brain activity associated with the same tennis-playing MI task used previously to detect activation in DOC patients [4]. Despite the limited number of detection channels, it was hypothesized that the enhanced depth sensitivity of TR-NIRS would provide robust detection of MI activation by strategic placement of the probes over motor planning regions, given these regions show the most consistent activation [2,31]. This hypothesis was tested on healthy participants by also acquiring fMRI data, which was used as a benchmark for calculating the sensitivity and precision of the fNIRS method.

2. Methods

2.1 Experimental protocol

Fifteen healthy subjects (5 females, aged 22 to 34 years with mean age = 26, all right handed) with no history of any neurological or psychiatric disorders were recruited for the study. All subjects provided written consent and were compensated for their participation in the study. The study was approved by the Research Ethics Board at Western University.

The experimental design consisted of participants performing the MI task in two separate blocks: one in the MRI scanner and the other in a research lab that housed the TR-fNIRS system. The order of data acquisition by the two modalities was randomized to avoid possible training effects, with 8 subjects performing the task first in the MRI scanner. The delay between the two acquisitions was between 15 minutes and an hour. The MI protocol consisted of 30 s alternating blocks of rest and tennis imagery, for a total acquisition time of 330 s [2,32]. During the task, participants were asked to remain as still as possible and to imagine hitting a tennis ball repeatedly as if they were playing a vigorous game of tennis. The cue words used to indicate the start of imagery and rest periods were “tennis” and “rest”, respectively.

2.1 Data acquisition and analysis

fMRI

Imaging data were acquired on a 3 Tesla (T) Biograph mMR scanner (Siemens Healthcare, Erlangen, Germany) using a 32-channel receive-only head coil. High-resolution T1-weighted magnetization prepared rapid gradient echo (MPRAGE) images (TR = 2000 ms, TE = 2.98 ms, FA = 9°, voxel size = 1x1x1 mm) were acquired for anatomical registration of the fMRI images. The functional data were acquired with an echo-planar imaging (EPI) sequence (TR = 3000 ms, TE = 30 ms, FA = 90°, slice thickness = 3 mm, voxel size = 3x3x3 mm). A noise attenuating MRI-compatible headset was used to present the verbal cues to the participants regarding the start of the alternative rest and task periods.

The functional images were pre-processed and analyzed using SPM8 (Wellcome Trust Center for Neuroimaging, University College London, UK). The scans were realigned to correct for motion artifacts, spatially normalized to the EPI template in SPM8, and smoothed with an 8-mm full width half maximum (FWHM) Gaussian kernel. Image data were filtered using a high-pass filter with a cut-off period of 128 s to remove slow signal drifts in the time-series. Single subject analysis based on the general linear model (GLM) was performed using the canonical hemodynamic response function. The condition of each scan was defined as belonging to either MI or rest condition.

Statistically significant brain activity was determined by whole-brain analysis with the statistical threshold set to a false discovery rate (FDR) corrected $p = 0.05$. For subjects who presented with no activation at the whole-brain level, small volume correction was performed using two 20-mm spheres placed over regions in the SMA and PMC, with the statistical threshold set to Family Wise Error (FWE) corrected $p = 0.05$. The location of each sphere was set based on the group average of the subjects that showed activity at the whole-brain level ($n = 11$). This small volume approach was considered reasonable for avoiding the removal of data sets that did not reach statistical significant at the more conservative whole-brain level given the *a prior* knowledge of the brain regions activated during MI [33,34].

Group level analysis was also performed for all participants that showed activity at the whole-brain level. SVC was used with the statistical threshold set to FWE $p < 0.05$ on 10-mm spherical ROIs centered on coordinates previously documented for the SMA, pre-SMA, dorsal PMC and the inferior parietal lobule [33].

fNIRS

The TR-fNIRS system was designed and built in-house, and it has been described in detail elsewhere [32,35,36]. These experiments used two picosecond pulsed lasers emitting at 760 and 830 nm at a pulse repetition rate of 80 MHz (PicoQuant, Berlin, Germany). The output powers from the laser heads were attenuated using neutral density filters (NDC-50-4M, Thorlabs, Newton, NJ, United States) in order to adjust the power delivered to the participant's head. An objective lens (NA = 0.25, magnification 10X, Olympus, Japan) was used to couple the light pulses from the laser head into a 1.5 m long multimode bifurcated fiber (ϕ = 0.4 mm, NA = 0.22, Fiberoptics Technology, Pomfret, Connecticut, United States). One emission fiber and four detection fiber bundles (ϕ = 3.6 mm, NA = 0.55, Fiberoptics Technology, Pomfret, Connecticut, United States) were secured on the head using an fNIRS cap built in-house [32]. The emission fiber was placed over the FCz location, according to the international 10-20 system. Each detector was placed 3 cm from the emitter in a cross formation (see Fig. 1). This orientation was chosen to record light that interrogated the SMA and PMC in each hemisphere. The placement of the detection channels was consistent across subjects with channel 1 placed posterior to the emission fiber, channel 2 on the left hemisphere, channel 3 anterior to the emission fiber, and channel 4 on the right hemisphere. The diffusively reflected light from the surface of the head was delivered to hybrid photomultiplier tubes (PMA Hybrid 50, PicoQuant, Berlin, Germany) via fiber bundles. A HydraHarp 400 (PicoQuant, Berlin,

Germany) time-correlated single-photon counting unit was used to record the arrival times of the photons and DTOFs were built using LabView software.

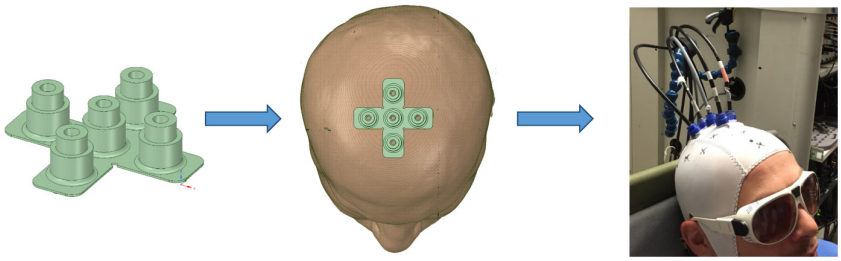

Fig. 1. Optode holder used to collect light from bilateral SMA and PMC and a picture of a participant showing the cap and probe locations for the MI experiment.

DTOFs were continuously acquired with a sampling interval of 300 ms throughout the 330 s min of the activation paradigm. For moment analysis, the lower and upper integration limits were set to 10% and 1% of the arrival time corresponding to the peak of the DTOF, respectively [37]. The first three moments – number of photons N, mean time of flight $\langle t \rangle$, and variance V – were calculated as outlined in reference [30]. The corresponding time series for each moment was processed using functions adapted from the SPM-fNIRS toolbox. First, each time course was corrected for motion artifacts using the MARA approach [38] and filtered using a fourth order Butterworth band-stop filter with stop-band frequencies between 0.08 and 1.5 Hz. The time courses were detrended to remove any slow signal drifts and smoothed using a hemodynamic response function with a FWHM of 4 s. Only the time courses for absorption changes at 830 nm were analyzed as this wavelength is more sensitive to the larger oxyhemoglobin changes [39]. Statistically significant signal changes were determined by fitting the general linear model to a time series ($p < 0.05$). This was performed for each of the three moments for every detection channels. FDR correction was applied to account for multiple comparisons (12 per subject: 4 channels, 3 moments each).

Sensitivity and precision were calculated by comparing the occurrence of activation detected by moment analysis and by fMRI. With this approach, the fMRI results were accepted as the ground truth. That is, a subject that showed activation by both fMRI and fNIRS was regarded as a true positive (TP) and a subject that showed no activation by both modalities as a true negative (TN). A false positive (FP) was defined as a subject that showed activation by fNIRS only, while a false negative (FN) was a subject that showed fMRI activation only.

The contrast-to-noise ratio (CNR) was calculated for each time series that showed significant activation. It was defined as the difference between the median task and rest signals divided by the median absolute deviation of the rest signal. The results were averaged across subjects and channels to obtain overall CNR estimates for N, $\langle t \rangle$ and V. Finally, the absorption coefficient values at 760 and 830 nm were calculated using the mean time of flight sensitivity factor and the $\langle t \rangle$ signals [30]. These values were then used to derive the median changes in the concentrations of oxy- and deoxy-hemoglobin during MI.

3. Results

Functional NIRS and fMRI data from one participant for whom robust activation was detected by both techniques is presented in Fig. 2. Displayed are the N, $\langle t \rangle$ and V time-series from channel 3 (anterior to the emission probe) and the corresponding GLM fit. A significant decrease in N, $\langle t \rangle$ and V was found during MI periods, reflecting the increased oxyhemoglobin concentration caused by functional hyperemia. In this example, all three moments showed significant task-related signal changes. The corresponding fMRI results exhibited robust activity in the PMC, SMA and regions of the parietal cortex at the whole-brain level. The fMRI time course for one voxel shows the expected increase in the BOLD signal during the task periods.

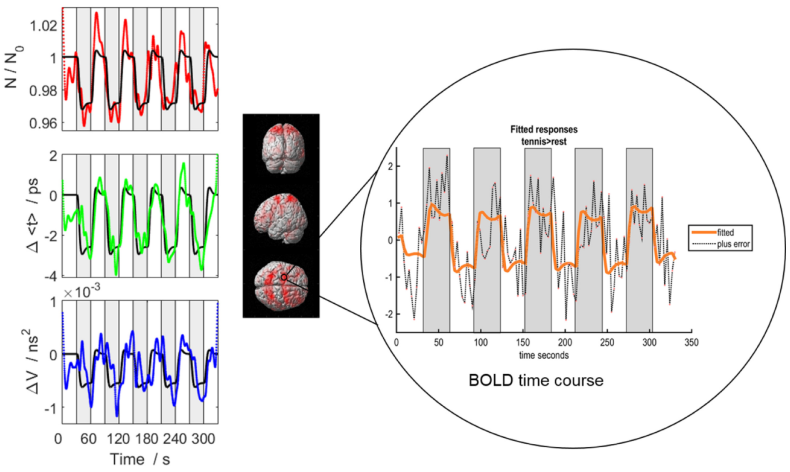

Fig. 2. Functional activation data from one subject. (Left) The time courses of all three moments – *N* (red), <*t*> (green) and *V* (blue) – are shown for the same channel. The black line in each graph is the best fit of the GLM model. The grey boxes indicate the periods of MI. (Right) The fMRI activation results were overlaid on the single subject rendered image in SPM with the BOLD time course from one voxel [-20, 0, 68] shown.

Figure 3 presents the fMRI and fNIRS results from all 15 subjects. The majority of the activation maps generated by fMRI were determined at the whole-brain level (FDR, $p < 0.05$); however, small volume correction was used for subjects 1, 12 and 13 (FWE, $p < 0.05$). Significant brain activity was detected in 13 of 15 subjects by both modalities, with activation consistently observed by fMRI in the SMA and/or the PMC. For fNIRS, channels 2 and 4, which were located on the left and right hemispheres respectively, provided the most consistent activation across subjects. In subject 3, activation was only detected in the variance time series of one channel, while subject 10 showed no fNIRS activation despite showing significant activation by fMRI.

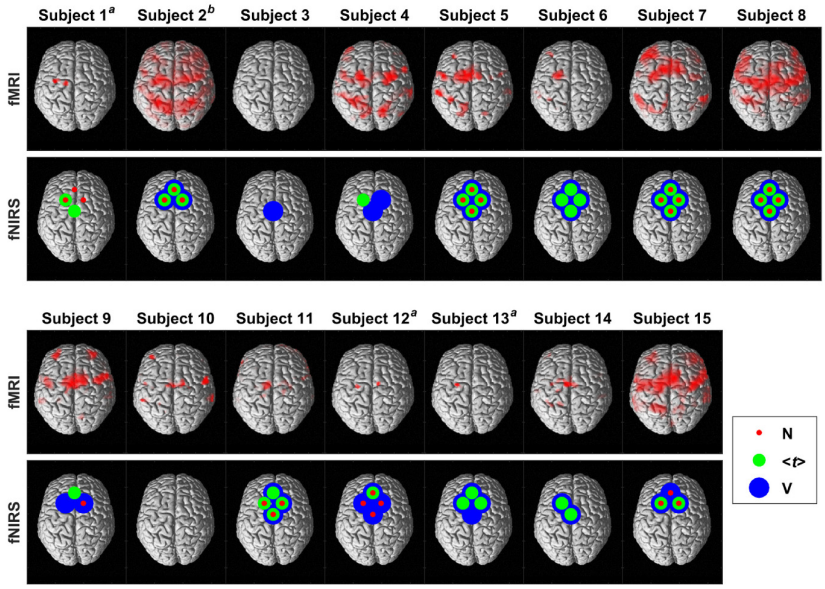

Fig. 3. fMRI and fNIRS results for all 15 subjects plotted on a single subject rendered image with the dorsal view shown. The red, green and blue circles indicate significant fNIRS activation detected by *N*, <*t*> and *V*, respectively. [a]fMRI results presented are after applying SVC. For display purposes, the results are thresholded at an uncorrected $p < 0.001$. [b]fNIRS results for subject 2 were only from 3 channels due to a technical issue with the 4th channel during the experiment.

The TR-fNIRS sensitivity and precision calculations for each of the individual moments (*N*, <*t*> and *V*) are presented in Table 1. The <*t*> and *V* had higher numbers of true positives compared to *N*, which is reflected in the higher sensitivity values. On the other hand, the precision estimates for all moments was high as only one FP was detected by *V*. The mean CNR for each moment was as follows: $N = 5.9 \pm 5.6$, $\langle t \rangle = 5.2 \pm 4.0$ and $V = 4.0 \pm 2.9$.

Table 1. Sensitivity and precision measurements for *N*, <*t*> and *V*. TP = true positive, FP = false positive, FN = false negative and TN = true negative.

	N (TP = 9, FN = 5, TN = 1, FP = 0)	<*t*> (TP = 13, FN = 1, TN = 1, FP = 0)	*V* (TP = 12, FN = 2, TN = 0, FP = 1)
Sensitivity[1]	64%	93%	86%
Precision[2]	100%	100%	92%

[1]*Sensitivity = TP / (TP + FN);* [2]*Precision = TP / (TP + FP)*

The time courses of oxy- and deoxy-hemologin showed the expected changes with increased oxy-hemologin and decreased deoxy-hemoglobin during MI activation (Fig. 4).

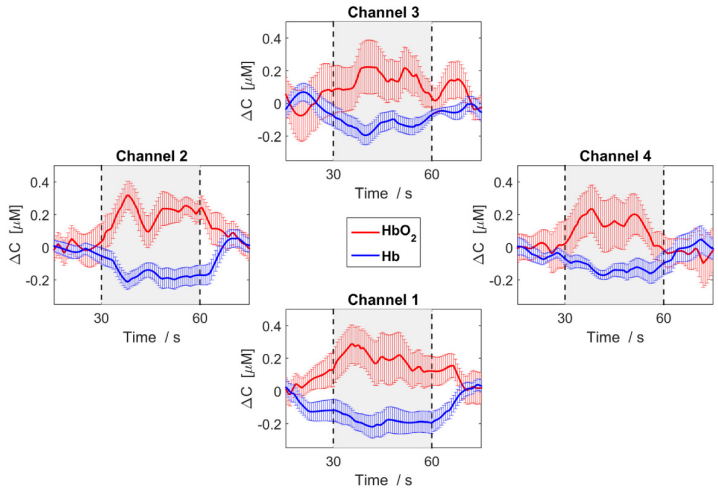

Fig. 4. Median change in concentration (ΔC) of oxy-hemoglobin (red) and deoxy-hemoglobin (blue) across participants that showed activity and averaged across the task cycles. The error bars represent the standard error of the median across subjects.

The group-wise fMRI analysis for all subjects who showed activation at the whole-brain level revealed significant activity in regions of the SMA, dorsal PMC, pre-SMA and inferior parietal lobule. The coordinates of the peak voxels in each cluster within the predefined ROIs are given in Table 2. For illustration purposes, whole-brain activation is presented in Fig. 5 with the statistical threshold set to an uncorrected $p < 0.001$.

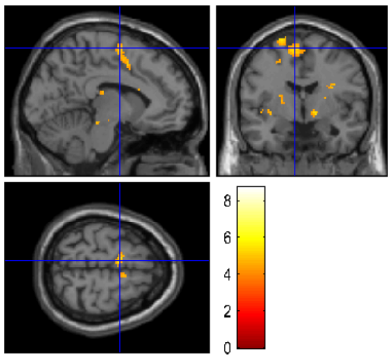

Fig. 5. Group-wise fMRI results from 11 participants that showed activity at the whole-brain level. The results are plotted on a canonical single subject T1 image. For display purposes, the results are thresholded at an uncorrected $p < 0.001$ at the whole-brain level.

Table 2. Brain regions that showed significant activity at the group-wise level (FWE corrected p<0.05) during MI using SVC

	MNI coordinates				
Brain area	x	y	z	Z score	*p* value
Pre-SMA	10	2	62	3.45	0.007
Dorsal PMC	-30	-8	52	3.50	0.017
	46	2	54	3.45	0.026
SMA	-6	-4	64	3.69	0.002
Inferior parietal lobule	-46	-34	28	3.45	0.026

4. Discussion

The aim of this study was to assess the ability of fNIRS to detect MI activation consistently across a group of healthy participants in order to assess its validity for translation to DOC patients. The rationale for conducting a control study was based on previous studies showing that the signal change associated with MI is less than that for corresponding motor execution tasks [20,21] and there can be considerable inter-subject variability, in part because of inverse oxy-hemoglobin responses measured with some participants [14,21]. A further consideration is that MI blood oxygenation level dependent (BOLD) activation is not always detectable in all subjects; a recent fMRI study by our group found no activation in 20% of healthy participants [2]. Although the lack of MI activity in some subjects has been based on physiological (e.g. magnitude of the alpha rhythms), or psychological (e.g. kinesthetic MI scores) factors [40], there remains no definitive reason as to why this occurs. Therefore, for the current study independent confirmation of MI activation was achieved by having subjects perform the same tennis-imagery task during an fMRI session.

Significant activation in the SMA and/or the PMC – areas known to be involved with the kinesthetic component MI [41] – was detected by fMRI in all but one of the 15 subjects, albeit it was necessary to use small-volume correction in three cases. Detecting activation in each subject by fNIRS was based on finding a statically significant signal decrease for at least one of the four optodes since they were all positioned over motor planning regions. Based on this criterion, the fNIRS and fMRI results were in good agreement, with discordance in only two cases. The overall agreement demonstrates the ability of fNIRS to detect MI activation on a single subject basis despite using a NIRS system with a limited number of optodes and the inherent uncertainties in probe placement based solely on the 10-20 system. This confirms our hypothesis that strategic placement of the probes would be sufficient for detecting tennis imagery activation considering previous studies have shown that the most robust activation is found in motor planning areas [33]. The choice of these areas, as opposed to focusing on the primary

motor cortex (M1) [11,42,43], was also confirmed by the fMRI results that showed no significant M1 activation at the group level. Individually, M1/parietal lobe activation was found in six participants, but the M1 component was inconsistent across participants and considerably smaller than activation in the secondary motor regions. This variability agrees with previous studies that also reported variable M1 activation with MI tasks [31,44,45]. The parietal lobe activity did reach statistical significance at the group-wise level and is likely associated with the visual component of MI [41].

A potential concern with using only a few optodes is adequate removal of signal changes in the scalp, which is frequently performed by adding closely spaced optodes that are sensitive to superficial tissue [46]. In this study, TR detection was used as an alternative means of reducing scalp contamination and enhancing the sensitivity to brain activity. This emerging technology has been used in a number of fNIRS studies involving motor and cognitive tasks [47], however, to the best of our knowledge, this is the first study involving MI. The improvement in detecting MI activity achieved by using TR-NIRS was assessed by calculating the sensitivity and precision of each of the first three statistical moments (N, $\langle t \rangle$ and V) using the fMRI results for comparison. It was expected that the higher moments ($\langle t \rangle$ and V) would perform better given their greater depth sensitivity [30], which has been shown to reduce the effects of task-related changes in scalp blood flow [17]. This was confirmed by the results given in Table 1 showing lower numbers of false negatives for $\langle t \rangle$ and V compared to that for N, which translated into better sensitivity values for the higher moments. The trade-off with weighting the signal to late-arriving photons is a reduction in the overall signal-to-noise ratio, as indicated by the inverse relationship between the activation-related CNR and moment order. This likely explains why consistent agreement between significant signal changes obtained by the $\langle t \rangle$ and V analyses for a specific optode was only found in 50% of participants. In most of the other cases, such as subjects 4 and 9, MI was detected by both $\langle t \rangle$ and V, but the specific optodes were not always the same. The higher sensitivity and precision estimates for $\langle t \rangle$ compared to V suggests that the former represents a good compromise between detection ability and CNR.

Another consideration with fNIRS is the presence of Mayer waves, which are spontaneous blood pressure oscillations around 0.1 Hz that can negatively impact the ability to detect activation-related oxygenation changes [18]. To investigate this potential effect in the current study, Mayer wave amplitude analysis was conducted on the pre-task data for each channel and moment (i.e. each statistical moment's time course before preprocessing). The amplitude of the Mayer wave was calculated from the power spectrum for frequencies between 0.06 and 0.14 Hz, as proposed by Yücel et al. [18]. The data were grouped into activated and inactivated channels for each moment since Mayer wave amplitude has been shown to vary across channels [18]. While the mean amplitude for the inactivated channels was higher than for the activated channels, this difference did not reach statistical significance.

Two previous fNIRS studies reported a high incidence of inverted NIRS signals during MI (between 40 to 60%), which was attributed to an inverse oxygenation response [14,21]. In contrast, the fNIRS results presented in Fig. 3 were based on the assumption that the signal at 830 nm would decrease during activation due to an increase in the oxy-hemoglobin concentration. This relationship was confirmed by converting the average $\langle t \rangle$ and V time courses across subjects into the corresponding changes in oxy- and deoxy-hemoglobin, as shown in Fig. 4. Similarly, the fMRI activation maps were generated assuming a signal increase with activation (i.e. a hyperemic response leading to greater blood oxygenation). The discrepancy between studies may be related to differences in MI tasks, location of the probes with regards to motor planning regions, and NIRS systems as Kempny et al. and Holper et al. both used multichannel continuous-wave devices [14,21] without correcting for extracerebral blood flow changes. Although the results of the current study cannot explain this discrepancy, this is an important issue regarding the confidence in using fNIRS as a BCI and warrants further investigation.

There are a number of limitations with this study. First, electromyography was not used to monitor for muscle movement. The lack of M1 activation detected by fMRI in

any of the subjects indicates that movement was minimal. However, including electromyography would be valuable in future studies involving only fNIRS. Second, fNIRS and fMRI were not acquired simultaneously because of technical challenges. The NIRS components are not MR compatible and would require long optical fibres (of the order of 6 to 8 m). The substantial increase in instrument dispersion would cause a temporal smearing of the measured DTOFs, hampering the ability to separate early and late arrival times [24]. The overall agreement between the fNIRS and fMRI results suggests that most subjects were able to perform the MI in both sessions. Moreover, we have previously reported consistent MI activation across imaging sessions [2]. However, variability in task performance cannot be completely ruled out as an explanation for the between-modality disagreement for subject 3 (classified as a false positive by V analyses) and subject 10 (classified as a false negative by all three moments). Given that MI activation is not observed in all people [2], subject 3′s fMRI results were not unexpected and the false positive categorization is likely correct considering the NIRS activation was based on a single moment from one optode. On the other hand, subject 10 showed robust fMRI activation that was not based on small-volume correction, but completely lacked any detectable fNIRS activation. Without simultaneous acquisition, this subject's classification as a false negative must remain.

A final consideration is that only using data from the 830-nm channel was used to detect MI-related activity. With continuous-wave fNIRS systems, both oxy and deoxy hemoglobin signals are frequently used in the statistical model as a means of controlling for potential scalp effects [16]. In the current study, moment analysis was used to enhance depth sensitivity, which is a simple approach for analyzing time-resolved data that could be easily used in BCI applications. To investigate the possibility of scalp contamination with this approach, GLM analysis was repeated using the oxy- and deoxy-hemoglobin signals derived from the mean time of flight data for both channels. This analysis resulted in activation detected in the same subjects as determined from the 830-nm channel alone.

5. Conclusion

This study demonstrated the ability of TR-fNIRS to detect brain activity during MI in healthy subjects, suggesting this optical technology is well suited to act as a BCI for DOC patients. The greater sensitivity shown by the higher moment analysis underlines the advantages of TR detection. It should be noted that moment analysis is relatively simple and could be easily incorporated into real time BCI algorithms. Furthermore, the development of small lasers and detectors that can be placed directly in contact with the skin highlight the possibility of building compact, low-cost TR-fNIRS systems that could be readily distributed to DOC patients [48].

Funding

Canada Excellence Research Chairs (CERC) program and the Natural Science and Engineering Research Council (NSERC) of Canada.

Acknowledgments

The authors would like to thank Ms. Tracy Ssali for her help with the fMRI data analysis, Ms. Heather Biernaski and Mr. John Butler for their help with running the MRI scanner.